Spring temperature variability over Turkey since 1800 CE reconstructed

from a broad network of tree-ring data

Nesibe Köse[(1),*]**, H. Tuncay Güner**[(1)]**, Grant L. Harley**[(2)]**, Joel Guiot**[(3)]

[(1)]Istanbul University, Faculty of Forestry, Forest Botany Department 34473 Bahçeköy-Istanbul, Turkey
[(2)]University of Southern Mississippi, Department of Geography and Geology, 118 College Drive Box 5051, Hattiesburg, Mississippi, 39406, USA
[(3)] Aix-Marseille Université, CNRS, IRD, CEREGE UM34, ECCOREV, 13545 Aix-en-Provence, France

*Corresponding author.   Fax: +90 212 226 11 13
 E-mail address: nesibe@istanbul.edu.tr

Abstract

The meteorological observational period in Turkey, which starts *ca.* 1930 CE, is too short for understanding long-term climatic variability. Tree rings have been used intensively as proxy records to understand summer precipitation history of the region, primarily because of having a dominant precipitation signal. Yet,, the historical context of temperature variability is unclear. Here we used higher order principle components of a network of 23 tree-ring chronologies to provide a high-resolution spring (March–April) temperature reconstruction over Turkey during the period 1800–2002. The reconstruction model accounted for 67% (Adj. $R^2 = 0.64$, $p < 0.0001$) of the instrumental temperature variance over the full calibration period (1930–2002). The reconstruction is punctuated by a temperature increase during the 20th century; yet extreme cold and warm events during the 19th century seem to eclipse conditions during the 20th century.. We found significant correlations between our March–April spring temperature reconstruction and existing gridded spring temperature reconstructions for Europe over Turkey and southeastern Europe. Moreover, the precipitation signal obtained from the tree-ring network (first principle component) showed highly significant correlations with gridded summer drought index reconstruction over Turkey and Mediterranean countries. Our results showed that, beside the dominant precipitation signal, a temperature signal can be extracted from tree-ring series and they can be useful proxies to reconstruct past temperature variability.

KEYWORDS: Dendroclimatology, Climate reconstruction, *Pinus nigra,* Principle component analysis, Spring temperature.

1 Introduction

An extensive body of literature details climate changes in the Mediterranean region over the last two millennia (*c.f.* Lionello, P. (Ed.), 2012). Paleolimnological studies provide evidence that the Medieval Climatic Anomaly (MCA; 900–1300 CE) characterized warm and dry conditions over the Iberian Peninsula, while the Little Ice Age (LIA; 1300–1850 CE) brought opposite climate conditions, forced by interactions between the East Atlantic and North Atlantic Oscillation (Sanchez-Lopez et al. 2016). In addition, Roberts et al. (2012) highlighted an intriguing spatial dipole NAO pattern between the western and eastern Mediterranean region, which brought anti-phased warm (cool) and wet (dry) conditions during the MCA and LIA. The hydro-climate patterns revealed by previous investigations appear to have been forced not only by NAO, but other climate modes with non-stationary teleconnections across the region (Roberts et al. 2012).

Significant decreases in spring diurnal temperature ranges (DTR) occurred throughout Turkey from 1929 to 1999 (Turkes & Sumer 2004). This decrease in spring DTRs was characterized by day-time temperatures that remained relatively constant while a significant increase in night-time temperatures were recorded over western Turkey and were concentrated around urbanized and rapidly-urbanizing cities. The historical context of this gradual warming trend in spring temperatures is unclear as the high-quality meteorological records in Turkey, which start in 1930s, are relatively short for understanding long-term climatic variability.

63   Tree rings have shown to provide useful information about the past climate of Turkey and were

64   used intensively during the last decade to reconstruct precipitation in the Aegean (Griggs et al.

65   2007), Black Sea (Akkemik et al. 2005, 2008; Martin-Benitto et al. 2016), Mediterranean regions

66   (Touchan et al. 2005a), as well as the Sivas (D'Arrigo & Cullen 2001), southwestern (Touchan et

67   al. 2003, Touchan et al. 2007; Köse et al. 2013), south-central (Akkemik & Aras 2005) and

68   western Anatolian (Köse et al. 2011) regions of Turkey. These studies used tree rings to

69   reconstruct precipitation because available moisture is often found to be the most important

70   limiting factor that influences radial growth of many tree species in Turkey. These studies

71   revealed past spring-summer precipitation, and described past dry and wet events and their

72   duration. Recently, Cook et al. (2015) presented Old World Drought Atlas (OWDA), which is a

73   set of year by year maps of reconstructed Palmer Drought Severity Index from tree-ring

74   chronologies over the Europe and Mediterranean Basin. Heinrich et al. (2013) provided a winter-

75   to-spring temperature proxy for Turkey from carbon isotopes within the growth rings of

76   *Juniperus excelsa* M. Bieb. since AD 1125. Low-frequency temperature trends corresponding to

77   the end of Medieval Climatic Anomaly and Little Ice Age were identified in the record, but the

78   proxy failed to identify the recent warming trend during the 20th century. In this study, we

79   present a tree-ring based spring temperature reconstruction from Turkey and compare our results

80   to previous reconstructions of temperature and precipitation to provide a more comprehensive

81   understanding of climate conditions during the 19th and 20th centuries.

82

83   **2 Data and Methods**

84   2.1 Climate of the Study Area

85

86   The study area, which spans 36–42º N and 26–38º E, was based on the distribution of available

87   tree-ring chronologies. This vast area covers much of western Anatolia and includes the western

88   Black Sea, Marmara, and western Mediterranean regions. Much of this area is characterized by a

89   Mediterranean climate that is primarily controlled by polar and tropical air masses (Türkeş

90   1996a, Deniz et al. 2011). In winter, polar fronts from the Balkan Peninsula bring cold air that is

91   centered in the Mediterranean. Conversely, the dry, warm conditions in summer are dominated

92   by weak frontal systems and maritime effects. Moreover, the Azores high-pressure system in

93   summer and anticyclonic activity from the Siberian high-pressure system often cause below

94   normal precipitation and dry sub-humid conditions over the region (Türkeş 1999, Deniz et al.

95   2011). In this Mediterranean climate, annual mean temperature and precipitation range from 3.6

96   °C to 20.1 °C and from 295 to 2220 mm, respectively, both of which are strongly controlled by

97   elevation (Deniz et al. 2011).

98

99   2.2 Development of tree-ring chronologies

100

101   To investigate past temperature conditions, we used a network of 23 tree-ring site chronologies

102   (Fig. 1). Fifteen chronologies were produced by previous investigations (Mutlu et al. 2011,

103   Akkemik et al. 2008, Köse et al. unpublished data, Köse et al. 2011, Köse et al. 2005) that

104   focused on reconstructing precipitation in the study area. In addition, we sampled eight new

105   study sites and developed tree-ring time series for these areas (Table 1). Increment cores were

106   taken from living *Pinus nigra* Arnold and *Pinus sylvestris* L. trees and cross-sections were taken

107   from *Abies nordmanniana* (Steven) Spach and *Picea orientalis* (L.) Link trunks.

108

109   Samples were processed using standard dendrochronological techniques (Stokes & Smiley 1968,

110   Orvis & Grissino-Mayer 2002, Speer 2010). Tree-ring widths were measured, then visually

111   crossdated using the list method (Yamaguchi 1991). We used the computer program COFECHA,

112   which uses segmented time-series correlation techniques, to statistically confirm our visual

113   crossdating (Holmes 1983, Grissino-Mayer 2001). Crossdated tree-ring time series were then

114   standardized by fitting a 67% cubic smoothing spline with a 50% cutoff frequency to remove

115   non-climatic trends related to the age, size, and the effects of stand dynamics using the ARSTAN

116   program (Cook 1985, Cook et al. 1990a). These detrended series were then pre-whitened with

117   low-order autoregressive models to produce time series with a strong common signal and

118   without biological persistence. These series may be more suitable to understand the effect of

119   climate on tree-growth, even if any persistence due to climate might be removed by pre-

120   whitening. For each chronology, the individual series were averaged to a single chronology by

121   computing the biweight robust means to reduce the influences of outliers (Cook et al. 1990b). In

122   this research we used residual chronologies obtained from ARSTAN to reconstruct temperature.

123

124   The mean sensitivity, which is a metric representing the year-to-year variation in ring width

125   (Fritts 1976), was calculated for each chronology and compared. The minimum sample depth for

126   each chronology was determined according to expressed population signal (EPS), which we used

127   as a guide for assessing the likely loss of reconstruction accuracy. Although arbitrary, we

128   required the commonly considered threshold of EPS > 0.85 (Wigley et al. 1984; Briffa & Jones

129   1990).

130

131   2.3 Identifying relationship between tree-ring width and climate

132

133 We extracted high resolution monthly temperature and precipitation records from the climate

134 dataset CRU TS 3.23 gridded at 0.5º intervals (Jones and Harris 2008) from KNMI Climate

135 Explorer (http://climexp.knmi.nl) for 36–42 ºN, 26–38 ºE. The period AD 1930–2002 was

136 chosen for the analysis because it maximized the number of station records within the study area.

137

138 First, the climate-growth relationships were investigated with response function analysis (RFA)

139 (Fritts 1976) for biological year from previous October to current October using the

140 DENDROCLIM2002 program (Biondi & Waikul 2004). This analysis is done to determine the

141 months during which the tree-growth is the most responsive to temperature. RFA results showed

142 that precipitation from May to August and temperature in March and April have dominant

143 control on tree-ring formation in the area. Second, we produced correlation maps showing

144 correlation coefficients between tree-ring chronologies and the climate factors most important

145 for tree growth, which are May–August precipitation and March–April temperature, to find the

146 spatial structure of radial growth-climate relationship (St. George 2014, St. George and Ault

147 2014, Hellmann et al. 2016). For each site we used the closest gridded temperature and

148 precipitation values.

149

150   2.4 Temperature reconstruction

151

152 The climate reconstruction is performed by regression based on the principal component (PCs)

153 of the 23 chronologies within the study area. Principle Component Analysis (PCA) was done

154 over the entire period in common to the tree-ring chronologies. The significant PCs were

155 selected by stepwise regression. We combined forward selection with backward elimination

156 setting $p < 0.05$ as entrance tolerance and $p < 0.10$ as exit tolerance. The final model obtained

157 when the regression reaches a local minimum of the root mean squared error (RMSE). The order

158 of entry of the PCs into the model was PC_3, PC_{21}, PC_4, PC_{15}, PC_5, PC_{17}, PC_7, PC_9, PC_{10}. The

159 regression equation is calibrated on the common period (1930–2002) between robust temperature

160 time-series and the selected tree-ring series. Third, the final reconstruction is based on bootstrap

161 regression (Till and Guiot 1990), a method designed to calculate appropriate confidence intervals

162 for reconstructed values and explained variance even in cases of short time-series. It consists in

163 randomly resampling the calibration datasets to produce 1000 calibration equations based on a

164 number of slightly different datasets.

165

166 The quality of the reconstruction is assessed by a number of standard statistics. The overall

167 quality of fit of reconstruction is evaluated based on the determination coefficient (R^2), which

168 expresses the percentage of variance explained by the model and RMSE, which expresses the

169 calibration error. This does not insure the quality of the extrapolation which needs additional

170 statistics based on independent observations, i.e. observations not used by the calibration

171 (verification data). They are provided by the observations not resampled by the bootstrap

172 process. The prediction RMSE (called RMSEP), the reduction of error (RE) and the coefficient

173 of efficiency (CE) are calculated on the verification data and enable to test the predictive quality

174 of the calibrated equations (Cook et al. 1994). Traditionally, a positive RE or CE values means a

175 statistically significant reconstruction model, but bootstrap has the advantage to produce

176 confidence intervals for such statistics without theoretical probability distribution and finally we

177 accept the RE and CE for which the lower confidence margin at 95% are positive. This is more

178 constraining than just accepting all positive RE and CE. For additional verification, we also

179 present traditional split-sample procedure results that divided the full period into two subsets of

180 equal length (Meko and Graybill 1995).

181

182 To identify the extreme March–April cold and warm events in the reconstruction, standard

183 deviation (SD) values were used. Years one and two SD above and below the mean were

184 identified as warm, very warm, cold, and very cold years, respectively., As a way to assess the

185 spatial representation of our temperature reconstruction, we conducted a spatial field correlation

186 analysis between reconstructed values and the gridded CRU TS3.23 temperature field (Jones and

187 Harris 2008) for a broad region of the Mediterranean over the entire instrumental period (ca.

188 1930–2002).   Finally, we compared our temperature reconstruction and also precipitation signal

189 (PC1) against existing gridded temperature and hydroclimate reconstructions for Europe over the

190 period 1800–2002. We performed spatial correlation analysis between [1] our temperature

191 reconstruction and gridded temperature reconstructions for Europe (Xoplaki et al. 2005,

192 Luterbacher et al. 2016) and OWDA (Cook et al. 2015); and [2] PC1 and summer precipitation

193 reconstruction (Pauling et al., 2006) and Old World Drought Atlas (OWDA) (Cook et al. 2015).

194

195 **2 Results and Discussion**

196   2.1 Tree-ring chronologies

197 In addition to 15 chronologies developed by previous studies, we produced six *P. nigra*, one *P.*

198 *sylvestris*, one *A. nordmanniana / P. orientalis* chronologies for this study (Table 2). The Çorum

199 district produced two *P. nigra* chronologies: one the longest (KAR; 627 years long) and the other

200 the most sensitive to climate (SAH; mean sensitivity value of 0.25). Previous investigations of

201   climate-tree growth relationships reported a mean sensitivity range of 0.13–0.25 for *P. nigra* in

202   Turkey (Köse 2011, Akkemik et al. 2008). The KAR, SAH, and ERC chronologies (with mean

203   sensitivity values from 0.22 to 0.25) were classified as very sensitive, and the SAV, HCR, and

204   PAY chronologies (mean sensitivity values range 0.17–0.18) contained values characteristic of

205   being sensitive to climate. The lowest mean sensitivity value was obtained for the ART *A.*

206   *nordmanniana / P. orientalis* chronology. Nonetheless, this chronology retained a statistically

207   significant temperature signal ($p < 0.05$).

208

209   2.2 Tree-ring growth-climate relationship

210   RFA coefficients of May to August precipitation are positively correlated with most of the tree-

211   ring series (Fig. 2) and among them, May and June coefficients are generally significant. The

212   first principal component of the 23 chronologies, which explains 47% of the tree-growth

213   variance, is highly correlated with May–August total precipitation, statistically ($r = 0.65$, $p <$

214   0.001) and visually (Fig. 3). The high correlation was expected given that numerous studies also

215   found similar results in Turkey (Akkemik 2000a, Akkemik 2000b, Akkemik 2003, Akkemik et

216   al. 2005, Akkemik et al. 2008, Akkemik & Aras 2005, Hughes et al. 2001, D'Arrigo & Cullen

217   2001, Touchan et al. 2003; Touchan et al. 2005a, Touchan et al. 2005b, Touchan et al. 2007,

218   Köse et al. 2011, Köse et al. 2012, Köse et al. 2013, Martin-Benitto et al. 2016). The influence

219   of temperature was not as strong as May–August precipitation on radial growth, although

220   generally positive in early spring (March and April) (Fig. 2). Conversely, the ART chronology

221   from northeastern Turkey contained a strong temperature signal, which was significantly positive

222   in March.

223   Correlation maps representing influence of May-August precipitation (Fig. 4a) and March-April

224   temperature (Fig 4b) also showed that strength of the summer precipitation signal is higher and

225   significant almost all over the Turkey. Higher precipitation in summer has a positive effect on

226   tree-growth, because of long-lasting dry and warm conditions over the Turkey (Türkeş 1996b,

227   Köse et al. 2012). Spring precipitation signal are generally positive and significant only for four

228   tree-ring sites. The sites located at the upper distributions of the species are generally showed

229   higher correlations. The highest correlations obtained for *Picea/Abies* chronology (ART) from

230   the Caucasus, and for *Pinus nigra* chronology (HCR) from the upper (about 1900 m) and

231   southeastern distribution of the species. This black pine forest was still partly covered by snow

232   from previous year during the field work in fall. Higher temperatures in spring maybe cause

233   snow melt earlier and lead to produce larger annual rings. In addition to these chronologies, we

234   also used the chronologies that revealed the influence of precipitation, as well as temperature to

235   reconstruct March–April temperature.

236

237

238   2.3 March-April temperature reconstruction

239   The higher order PCs of the 23 chronologies are significantly correlated with the March–April

240   temperature and, by nature, are independent on the precipitation signal (Table 3). The best

241   selection for fit temperature are obtained with the PC_3, PC_4, PC_5, PC_7, PC_9, PC_{10}, PC_{15}, PC_{17},

242   PC_{21}, which explains together 25% of the tree-ring chronologies. So the temperature signal

243   remains important in the tree-ring chronologies and can be reconstructed. The advantage to

244   separate both signals through orthogonal PCs enable to remove an unwanted noise for our

245   temperature reconstruction. Thus, PC_1 was not used as potential predictor of temperature because

246   it is largely dominated by precipitation (Table 3, Fig. 3). The last two PCs contain a too small

247   part of the total variance to be used in the regressions. However, even if Jolliffe (1982) and Hadi

248   & Ling (1998) claimed that certain PCs with small eigenvalues (even the last one), which are

249   commonly ignored by principal components regression methodology, may be related to the

250   independent variable, we must be cautious with that because they may be much more dominated

251   by noise than the first ones. So, the contribution of each PC to the regression sum of squares is

252   also important for selection of PCs (Hadi & Ling 1998). The findings of Jolliffe (1982) and Hadi

253   & Ling (1998) provide a justification for using non-primary PCs, (*e.g*., of second and higher

254   order) in our regression, given that correlations with temperature may be over-powered by

255   affects from precipitation in our study area (Cook 2011, personal communication).

256

257   Using this method, the calibration and verification statistics indicated a statistically significant

258   reconstruction (Table 4, Fig. 5). For additional verification, we also present split-sample

259   procedure results. Similarly bootstrap results, the derived calibration and verification tests using

260   this method indicated a statistically significant RE and CE values (Table 5).

261

262   The regression model accounted for 67% (Adj. $R^2 = 0.64$, $p < 0.0001$) of the actual temperature

263   variance over the calibration period (1930–2002). Also, actual and reconstructed March–April

264   temperature values had nearly identical trends during the period 1930–2002 (Fig. 5). Moreover,

265   the tree-ring chronologies successfully simulated both high frequency and warming trends in the

266   temperature data during this period. The reconstruction was more powerful at classifying warm

267   events rather than cold events. Over the last 73 years, eight of ten warm events in the

268   instrumental data were also observed in the reconstruction, while five of nine cold events were

269   captured. Similarly, previous tree-ring based precipitation reconstructions for Turkey (Köse et al.

270   2011; Akkemik et al. 2008) were generally more successful in capturing dry years rather than

271   wet years.

272

273   Our temperature reconstruction on the 1800–2002 period is obtained by bootstrap regression,

274   using 1000 iterations (Fig. 6). The confidence intervals are obtained from the range between the

275   2.5^{th} and the 97.5^{th} percentiles of the 1000 simulations. For the pre-instrumental period (1800–

276   1929), a total of 23 cold (1813, 1818, 1821, 1824, 1837, 1848, 1854, 1858, 1860, 1869, 1877–

277   1878, 1880–1881, 1883, 1897–1898, 1905–1907, 1911–1912, 1923) and 13 warm (1801–1802,

278   1807, 1845, 1853, 1866, 1872–1873, 1879, 1885, 1890, 1901, 1926) events were determined.

279   After comparing our results with event years obtained from May–June precipitation

280   reconstructions from western Anatolia (Köse et al. 2011), the cold years 1818, 1848, and 1897

281   appeared to coincide with wet years and 1881 was a very wet year for the entire region.

282   Furthermore, these years can be described as cold (in March–April) and wet (in May–June) for

283   western Anatolia.

284

285   Among the warm periods in our reconstruction, conditions during the year 1879 were dry, 1895

286   wet, and 1901 very wet across the broad region of western Anatolia (Köse et al. 2011). Hence,

287   we defined 1879 as a warm (in March–April) and dry year (in May–June), and 1895 and 1901

288   were warm and wet years. In the years 1895 and 1901 the combination of a warm early spring

289   and a wet late spring-summer caused enhanced radial growth in Turkey, interpreted as longer

290   growing seasons without drought stress.

291

292 Of these event years, 1897 and 1898 were exceptionally cold and 1845, 1872 and 1873 were

293 exceptionally warm. During the last 200 years, our reconstruction suggests that the coldest year

294 was 1898 and the warmest year was 1873. The reconstructed extreme events also coincided with

295 accounts from historical records. Server (2008) recounted the winter of 1898 as characterized by

296 anomalously cold temperatures that persisted late into the spring season. A family, who brought

297 their livestock herds up into the plateau region in Kırşehir seeking food and water were suddenly

298 covered in snow on 11 March 1898. This account of a late spring freeze supports the

299 reconstruction record of spring temperatures across Turkey, and offers corroboration to the

300 quality of the reconstructed values.

301

302 Seyf (1985) reported that extreme summer temperature during the year 1873 resulted in

303 widespread crop failure and famine. Historical documents recorded an infamous drought-derived

304 famine that occurred in Anatolia from 1873 to 1874 (Quataert, 1996, Kuniholm, 1990), which

305 claimed the lives of 250,000 people and a large number of cattle and sheep (Faroqhi, 2009). This

306 drought caused widespread mortality of livestock and depopulation of rural areas through human

307 mortality, and migration of people from rural to urban areas. Further, the German traveler

308 Naumann (1893) reported a very dry and hot summer in Turkey during the year 1873 (Heinrich

309 et al, 2013). Conditions worsened when the international stock exchanges crashed in 1873

310 (Zürcher, 2004). Our temperature record suggests that dry conditions during the early 1870s

311 were possibly exacerbated by warm spring temperatures that likely carried into summer. A

312 similar pattern of intensified drought by warm temperatures was demonstrated recently by

313 Griffin and Anchukaitis (2014) for the current drought in California, USA.

314

315   Extreme cold and warm events were usually one year long, and the longest extreme cold and

316   warm events were two and three years, respectively. These results were similar with durations of

317   extreme wet and dry events in Turkey (Touchan et al. 2003, Touchan et al. 2005a, Touchan et al.

318   2005b, Touchan et al. 2007, Akkemik & Aras, 2005, Akkemik et al. 2005, Akkemik et al. 2008,

319   Köse et al. 2011, Güner et al. 2016). Moreover, seemingly innocuous short-term warm events,

320   such as the 1807 event, were recorded across the Mediterranean and in high elevations of the

321   European regions. Casty et al. (2005) reported the year 1807 as being one of the warmest alpine

322   summers in the European Alps over the last 500 years. As such, a drought record from Nicault et

323   al. (2008) echoes this finding, as a broad region of the Mediterranean basin experienced drought

324   conditions.

325

326   Low frequency variability of our spring temperature reconstruction showed larger variability in

327   nineteenth century than twentieth century. Similar results observed on previous tree-ring based

328   precipitation reconstructions from Turkey (Touchan et al. 2003, D'Arrigo et al. 2001, Akkemik

329   and Aras 2005, Akkemik et al. 2005, Köse et al. 2011). Moreover, cold (warm) periods observed

330   in our reconstruction are generally appeared as generally wet in the precipitation reconstructions,

331   while rarely correlated with dry (wet) periods (Fig. 7).   When we compare the relationship

332   between temperature and precipitation over the instrumental period, both case, cold (warm) and

333   wet (dry) as well as cold (warm) and dry (wet), can be observed.

334

335   Heinrich et al. (2013) analyzed winter-to-spring (January–May) air temperature variability in

336   Turkey since AD 1125 as revealed from a robust tree-ring carbon isotope record from *Juniperus*

337   *excelsa*. Although they offered a long-term perspective of temperature over Turkey, the

338   reconstruction model, which covered the period 1949–2006, explained 27% of the variance in

339   temperature since the year 1949. In this study, we provided a short-term perspective of

340   temperature fluctuation based on a robust model (calibrated and verified 1930–2002; Adj. $R^2 =$

341   0.64; $p < 0.0001$). Yet, the Heinrich et al. (2013) temperature record did not capture the 20th

342   century warming trend as found elsewhere (Wahl et al. 2010). However, their temperature trend

343   does agree with trend analyses conducted on meteorological data from Turkey and other areas in

344   the eastern Mediterranean region. The warming trend seen during our reconstruction calibration

345   period (1930–2002) was similar to the data shown by Wahl et al. (2010) across the region and

346   hemisphere. Further, the warming trends seen in our record agrees with data presented by Turkes

347   & Sumer (2004), of which they attributed to increased urbanization in Turkey. Considering long-

348   term changes in spring temperatures, the 19th century was characterized by more high-frequency

349   fluctuations compared to the 20th century, which was defined by more gradual changes and

350   includes the beginning of decreased DTRs in the region (Turkes & Sumer 2004).

351

352   **4 Comparison with instrumental gridded data and spatial reconstructions**

353

354   Spatial correlation analysis revealed that our network-based temperature reconstruction was

355   representative of conditions across Turkey, as well as the broader Mediterranean region (Fig. 8).

356   During the period 1930–2002, estimated temperature values were highly significant (r range 0.5–

357   0.6, $p < 0.01$) with instrumental conditions recorded from southern Ukraine to the west across

358   Romania, and from northern areas of Libya and Egypt to the east across Iraq. The strength of the

359   reconstruction model is evident in the broad spatial implications demonstrated by the

360   temperature record. Thus, we interpret warm and cold periods and extreme events within the

361   record with high confidence.

362

363   We compared our tree-ring based temperature reconstruction with existing gridded temperature

364   reconstructions for Europe (Xoplaki et al. 2005, Luterbacher et al. 2016) and the Old World

365   Drought Atlas (OWDA) (Cook et al. 2015) for further validation of the reconstruction (Fig. 9a,

366   b, c, respectively). Spatial correlations over the past 200 years were lower with reconstructed

367   European summer temperature (May to July) (Fig. 9b). Yet, we expected this result because of

368   the paucity of Turkey-derived proxies in the other reconstructions, as well as the differing

369   seasons involved across the reconstructions. Similarly, our reconstruction showed weak

370   correlations with summer drought index over Turkey. Beside comparing different seasons,

371   perhaps this is because less precipitation begets drought conditions rather than high temperature

372   in the region. The highest and significant ($p < 0.05$) correlations were found with European

373   spring (March to May) temperature reconstruction over southeastern Europe, which are stronger

374   over Turkey (Fig. 9a). We used the mean of corresponding grid points from European spring

375   temperature reconstruction over the study area (36–42º N, 26–38º E) to show how the correlation

376   changed over time (Fig. 10). The correlation coefficient was highly significant ($r = 0.76$, $p <$

377   0.001) during our calibration period (1930–2002). We found lower but still significant

378   correlation ($r = 0.35$, $p < 0.10$) for the period of 1901–1929, which climatic records are very few

379   over the region while available data has sufficient quality for most part of Europe. These results

380   give additional verification for our reconstruction. Moreover, our reconstruction has a weak,

381   insignificant relationship ($r = 0.13$, $p > 0.10$) during the 19th century. This may be related to poor

382   reconstructive skill of European spring temperature reconstruction over Turkey, which contains

383   few proxies from the country (Xoplaki et al. 2005, Luterbacher et al. 2004). Nonetheless, these

384   results demonstrate that tree-ring chronologies from Turkey can serve as useful temperature

385   proxies for further spatial temperature reconstructions to fill the gaps in the area.

386

387   We also compared the precipitation signal (PC1) obtained from our tree-ring network with Old

388   World Drought Atlas (OWDA) (Cook et al. 2015) and gridded European summer precipitation

389   reconstruction (Pauling et al., 2006) to test the strength of the signal spatially (Fig. 9d and e,

390   respectively). We calculated highly significant positive correlations with summer drought index

391   over Turkey and neighboring European countries such as Greece, Bulgaria, and Romania, while

392   significant correlations are lover for the other Mediterranean countries (Fig. 9d). We found lover

393   but still significant correlations over Turkey and Mediterranean countries with European summer

394   precipitation reconstruction (Fig. 9e). Pauling et al. (2006) stated that poor reconstructive skills

395   determined over Turkey because of few instrumental record before the1930s. These results

396   showed that summer precipitation signal represented by PC1 is very strong not only on

397   instrumental period, but also on pre-instrumental period, and represents a large spatial coverage.

398

399   **4 Conclusions**

400

401   In this study, we used a broad network of tree-ring chronologies to provide the first tree-ring

402   based temperature reconstruction for Turkey and identified extreme cold and warm events during

403   the period 1800–1929 CE. Similar to the precipitation reconstructions against which we compare

404   our air temperature record, extreme cold and warm years were generally short in duration (one

405   year) and rarely exceeded two-three years in duration. The coldest and warmest years over

406 western Anatolia were experienced during the 19th century, and the 20th century is marked by a

407 temperature increase.

408

409 Reconstructed temperatures for the 19th century suggest that more short-term fluctuations

410 occurred compared to the 20th century. The gradual warming trend shown by our reconstruction

411 calibration period (1930–2002) is coeval with decreases in spring DTRs. Given the results of

412 Turkes and Sumer (2004), the variations in short- and long-term temperature changes between

413 the 19th and 20th centuries might be related to increased urbanization in Turkey.

414

415 We highlight that the 20th century warming trend is unprecedented within the context of the past

416 *ca.* 200 years, especially over the past *ca.* 15 years. Correlations with gridded climate fields and

417 other climate reconstructions from the region revealed that our network-based temperature

418 reconstruction was representative of conditions across Turkey, as well as the broader

419 Mediterranean region. Expanding the tree-ring network across Turkey, especially to the east, will

420 improve the spatial implications of future temperature reconstructions.

421

422 The study revealed the potential for reconstructing temperature in an area previously thought

423 impossible, especially given the strong precipitation signals displayed by most tree species

424 growing in the dry Mediterranean climate that characterizes broad areas of Turkey. Our

425 reconstruction only spans 205 years due to the shortness of the common interval for the

426 chronologies used in this study, but the possibility exists to extend our temperature

427 reconstruction further back in time by increasing the sample depth with more temperature-

428 sensitive trees, especially from northeastern Turkey. Thus future research will focus on

429 increasing the number of tree-ring sites across Turkey, and maximizing chronology length at

430 existing sites that would ultimately extend the reconstruction back in time.

431

432 **Acknowledgements**

433

434 This research was supported by The Scientific and Technical Research Council of Turkey

435 (TUBITAK); Projects ÇAYDAG 107Y267 and YDABAG 102Y063. N. Köse was supported by

436 The Council of Higher Education of Turkey. We are grateful to the Turkish Forest Service

437 personnel and Ali Kaya, Umut Ç. Kahraman and Hüseyin Yurtseven for their invaluable support

438 during our field studies. We thank to Dr. Ufuk Turuncoğlu for his help on spatial analysis. J.

439 Guiot was supported by the Labex OT-Med (ANR-11-LABEX-0061), French National Research

440 Agency (ANR).

441

References

Akkemik, Ü.: Dendroclimatology of Umbrella pine (*Pinus pinea* L.) in Istanbul (Turkey), Tree-Ring Bull., 56, 17–20, 2000a.

Akkemik, Ü.: Tree-ring chronology of *Abies cilicica* Carr. in the Western Mediterranean Region of Turkey and its response to climate, Dendrochronologia, 18, 73–81, 2000b.

Akkemik, Ü.: Tree-rings of *Cedrus libani* A. Rich the northern boundary of its natural distribution, IAWA J, 24(1), 63-73, 2003.

Akkemik ,Ü and Aras, A.: Reconstruction (1689−1994) of April−August precipitation in southwestern part of central Turkey, Int. J. Clim., 25, 537−548, 2005.

Akkemik, Ü., Dagdeviren, N., and Aras, A.: A preliminary reconstruction (A.D. 1635−2000) of spring precipitation using oak tree rings in the western Black Sea region of Turkey, Int. J. Biomet., 49(5), 297−302, 2005.

Akkemik, Ü., D'Arrigo, R., Cherubini, P., Köse, N., and Jacoby, G.: Tree-ring reconstructions of precipitation and streamflow for north-western Turkey, Int. J. Clim., 28, 173−183, 2008.

Biondi, F. and Waikul, K.: DENDROCLIM2002: A C++ program for statistical calibration of climate signals in tree-ring chronologies, Comp. Geosci., 30, 303−311, 2004.

Briffa, K. R. and Jones, P. D.: Basic chronology statistics and assessment. In: Methods of Dendrochronology: Applications in the Environmental Sciences (Cook, E. and Kairiukstis, L. A. eds). Kluwer Academic Publishers, Amsterdam, pp. 137–152, 1990.

Casty, C., Wanner, H., Luterbacher, J., Esper, J., and Böhm, R.: Temperature and precipitation variability in the European Alps since 1500, Int. J. Clim., 25(14), 1855–1880, 2005.

463 Cook, E.: A time series analysis approach to tree-ring standardization. PhD. Dissertation.

464 University of Arizona, Tucson, 1985.

465 Cook, E., Briffa, K., Shiyatov, S., and Mazepa, V.: Tree-ring standardization and growth-trend

466 estimation. In: Methods of Dendrochronology: Applications in the Environmental Sciences

467 (Cook, E. and Kairiukstis, L. A. eds). Kluwer Academic Publishers, Amsterdam, pp.104–

468 122, 1990a.

469 Cook, E., Shiyatov, S., and Mazepa, V.: Estimation of the mean chronology. In: Methods of

470 Dendrochronology: Applications in the Environmental Sciences (Cook, E. and Kairiukstis, L.

471 A. eds). Kluwer Academic Publishers, Amsterdam, pp. 123–132, 1990b.

472 Cook, E.R, Seager R., et al.: Old World megadroughts and pluvials during the Common Era. Sci.

473 Adv., 1, e1500561, doi:10.1126/sciadv.1500561, 2015.

474 D'Arrigo, R. and Cullen, H. M.: A 350-year (AD 1628–1980) reconstruction of Turkish

475 precipitation. Dendrochronologia ,19(2), 169–177, 2001.

476 Deniz, A., Toros, T., and Incecik, S.: Spatial variations of climate indices in Turkey, Int. J.

477 Clim., 31, 394-403, 2011.

478 Fritts, H. C.: Tree Rings and Climate. Academic Press, New York, 1976.

479 Griggs, C., DeGaetano, A., Kuniholm, P., and Newton, M.: A regional high-frequency

480 reconstruction of May–June precipitation in the north Aegean from oak tree rings, A.D.

481 1809–1989, Int. J. Clim., 27, 1075–1089, 2007.

482 Grissino-Mayer, H. D.: Evaluating crossdating accuracy: A manual and tutorial for the computer

483 program COFECHA, Tree-Ring Res., 57, 205–221, 2001.

484 Griffin, D. and Anchukaitis, K. J.: How unusual is the 2012–2014 California drought? Geophy.

485   Res. Lett., 41(24), 9017–9023, 2014.

486 Güner, H.T., Köse, N., Harley, G. L.: 200-year reconstruction of Kocasu River (Sakarya River

487   Basin, Turkey) streamflow derived from a tree-ring network, Int. J. Biometeprol., DOI

488   10.1007/s00484-016-1223-y, 2016.

489 Hadi, A. S. and Ling, R. F.: Some cautionary notes on the use of principal components

490   regression, Amer. Statist., 52(1), 15–19, 1998.

491 Heinrich, I., Touchan, R., Liñán, I. D., Vos, H., and Helle, G.: Winter-to-spring temperature

492   dynamics in Turkey derived from tree rings since AD 1125, Clim. Dynam., 41(7–8), 1685–

493   1701, 2013.

494 Hellmann, L., Agafonov, L., et al.: Diverse growth trends and climate responses across Eurasia's

495   boreal forest. Environmental Research Letters: 11: 074021, doi:10.1088/1748-

496   9326/11/7/074021.

497 Holmes, R. L.: Computer-assisted quality control in tree-ring data and measurements, Tree-Ring

498   Bull., 43, 69–78, 1983.

499 Hughes, M. K., Kuniholm, P. I, Garfin, G. M., Latini, C., and Eischeid, J.: Aegean tree-ring

500   signature years explained, Tree-Ring Res., 57(1), 67–73, 2001.

501 Jolliffe, I. T.: A note on the use of principal components in regression, Appl. Stat., 31(3), 300–

502   303, 1982.

503 Jones, P. D. and Harris, I.: Climatic Research Unit (CRU) time-series datasets of variations in

504   climate with variations in other phenomena. NCAS British Atmospheric Data Centre, 2008.

505   http://catalogue.ceda.ac.uk/uuid/3f8944800cc48e1cbc29a5ee12d8542d

506   Köse, N., Akkemik, Ü., and Dalfes, H. N.: Anadolu'nun iklim tarihinin son 500 yılı:

507   Dendroklimatolojik ilk sonuçlar. Türkiye Kuvaterner Sempozyumu-TURQUA–V, 02–03

508   Haziran 2005, Bildiriler Kitabı, 136–142 (In Turkish), 2005.

509   Köse, N., Akkemik, Ü., Dalfes, H. N., and Özeren, M. S.: Tree-ring reconstructions of May–June

510   precipitation of western Anatolia, Quat. Res., 75, 438–450, 2011.

511   Köse, N., Akkemik, Ü., Dalfes, H. N., and Özeren, M. S., Tolunay D.: Tree-ring growth of Pinus

512   nigra Arn. subsp. pallasiana under different climate conditions throughout western Anatolia,

513   Dendrochronologia, 295-301, 2012.

514   Köse, N., Akkemik, U., Guner, H.T., Dalfes, H.N., Grissino-Mayer, H.D., Ozeren, M.S., Kindap,

515   T.: An improved reconstruction of May– June precipitation using tree-ring data from western

516   Turkey and its links to volcanic eruptions, Int. J. Biometeorol, 57(5), 691–701, 2013.

517   Lionello, P. (Ed.),:The Climate of the Mediterranean Region, from the Past to the Future.

518   Elsevier, Amsterdam, Netherlands, 2012.

519   Luterbacher, J., Dietrich, D., Xoplaki, E., Grosjean, M., Wanner, H.:European seasonal and

520   annual temperature variability, trends and extremes since 1500. Science, 303, 1499–1503,

521   2004.

522   Luterbacher, J., Werner, J.P., et al.: European summer temperatures since Roman times.

523   Environmental Research Letters, 11: 024001, doi:10.1088/1748-9326/11/1/024001, 2016.

524   Martin-Benito, D., Ummenhofer C.C., Köse, N., Güner, H.T., Pederson, N.: Tree-ring

525   reconstructed May-June precipitation in the Caucasus since 1752 CE, Clim. Dyn., DOI

526   10.1007/s00382-016-3010-1, 2016.

527   Meko, D. M. and Graybill, D. A.: Tree-ring reconstruction of upper Gila River discharge, Wat.

528   Res. Bull., 31, 605–616, 1995.

529   Mutlu, H., Köse, N., Akkemik, Ü., Aral, D., Kaya, A., Manning, S. W., Pearson, C. L., and

530   Dalfes, N.: Environmental and climatic signals from stable isotopes in Anatolian tree rings,

531   Turkey, Reg. Emviron. Change, doi: 10.1007/s1011301102732, 2011.

532   Nicault, A., Alleaume, S., Brewer, S., Carrer, M., Nola, P., and Guiot, J.: Mediterranean drought

533   fluctuation during the last 500 years based on tree-ring data, Clim. Dynam., 31(2–3), 227–

534   245, 2008.

535   Orvis, K. H. and Grissino-Mayer, H. D.: Standardizing the reporting of abrasive papers used to

536   surface tree-ring samples, Tree-Ring Res., 58, 47–50, 2002.

537   Pauling, A., Luterbacher, J., Casty, C., Wanner, H.: Five hundred years of gridded high-

538   resolution precipitation reconstructions over Europe and the connection to large-scale

539   circulation. Clim. Dynam., 26, 387–405, 2006.

540   Roberts, N., Moreno, A., Valero-Garces, B.L.: Palaeolimnological evidence for an east-west

541   climate see-saw in the Mediterranean since AD 900. Glob. Planet. Change, 84, 23–34, 2012.

542   Sanchez-López, G. Hernandez, A., Pla-Rabes, et al.: Climate reconstruction for the last two

543   millennia in central Iberia: The role of East Atlantic (EA), North Atlantic Oscillation (NAO)

544   and their interplay over the Iberian Peninsula. Quaternary Science Reviews,149, 135–150,

545   2016.

546   Server, M.: Evaluation of an oral history text in the context of social memory and traditional

547   activity, Milli Folklor 77, 61–68 (In Turkish), 2008.

548   Speer, J. H.: Fundamentals of Tree-Ring Research, University of Arizona Press, Tucson, 2010.

549   St. George, S.: An overview of tree-ring width records across the Northern Hemisphere, Quat.

550   Sci. Rev., 95, 132–150, 2014.

551 St. George, S., and Ault. T. R.: The imprint of climate within northern hemisphere trees, Quat.

552   Sci. Rev., 89, 1–4, 2014.

553 Stokes, M. A. and Smiley, T. L.: An Introduction to Tree-ring Dating, The University of Arizona

554   Press, Tucson, 1996.

555 Till, C. and Guiot, J.: Reconstruction of precipitation in Morocco since A D 1100 based on

556   *Cedrus atlantica* tree-ring widths, Quat. Res., 33, 337–351, 1990.

557 Touchan, R., Garfin, G. M., Meko, D. M., Funkhouser, G., Erkan, N., Hughes, M. K., and

558   Wallin, B. S.: Preliminary reconstructions of spring precipitation in southwestern Turkey

559   from tree-ring width, Int. J. Clim., 23, 157–171, 2003.

560 Touchan, R., Xoplaki, E., Funkhouser, G., Luterbacher, J., Hughes, M. K., Erkan, N., Akkemik,

561   Ü., and Stephan, J.: Reconstruction of spring/summer precipitation for the Eastern

562   Mediterranean from tree-ring widths and its connection to large-scale atmospheric

563   circulation, Clim. Dynam., 25, 75–98, 2005a.

564 Touchan, R., Funkhouser, G., Hughes, M. K., and Erkan, N.: Standardized Precipitation Index

565   reconstructed from Turkish ring widths, Clim. Change, 72, 339-353, 2005b.

566 Touchan, R., Akkemik, Ü., Huges, M. K., and Erkan, N.: May–June precipitation reconstruction

567   of southwestern Anatolia, Turkey during the last 900 years from tree-rings, Quat. Res., 68,

568   196-202, 2007.

569 Turkes, M.: Spatial and temporal analysis of annual rainfall variations in Turkey, Int. J. Clim.,

570   16, 1057–1076, 1996a.

571   Turkes, M.:. Meteorological drought in Turkey: a historical perspective, 1930−1993. In: Drought

572   Network News, International Drought Information Center, University of Nebraska, 8, pp. 17−

573   21, 1996b.

574   Turkes, M.: Vulnerability of Turkey to desertification with respect to precipitation and aridity

575   conditions. Turk. J. Engineer. Environ Sci., 23, 363–380, 1999.

576   Turkes, M. and Sumer, U. M.: Spatial and temporal patterns of trends variability in diurnal

577   temperature ranges of Turkey. Theor. Appl. Clim., 77, 195–227, 2004.

578   Xoplaki, E., Luterbacher J., Paeth H., Dietrich, D., Grosjean, M., Wanner, H.: European spring

579   and autumn temperature variability and change of extremes over the last half millennium.

580   Geophys. Res. Lett., 32, L15713, doi:10.1029/2005GL023424.

581   Wahl, E. R., Anderson, D. M., Bauer, B. A., Buckner, R., Gille, E. P., Gross, W. S., Hartman,

582   M., and Shah, A.: An archive of high-resolution temperature reconstructions over the past

583   two millennia, Geochem. Geophys. Geosyst., 11, Q01001, doi:10.1029/2009GC002817,

584   2010.

585   Wigley, T. M. L., Briffa, K. R., and Jones, P. D.: On the average value of correlated time series

586   with applications in dendroclimatology and hydrometeorology, J. Clim. Appl. Met., 23, 201–

587   213, 1984.

588   Yamaguchi, D. K.: A simple method for cross-dating increment cores from living trees. Can. J.

589   For. Res., 21, 414–416, 1991.

590   Zücher, E. J.: Turkey: A modern history. Oxford Publishing Services, New York, 2004.

591   Table 1. Site information for the new chronologies developed by this study in Turkey.

Site name	Site code	Species	No. trees/ cores	Aspect	Elev. (m)	Lat. (N)	Long. (E)
Çorum, Kargı, Karakise kayalıkları	KAR	*Pinus nigra*	22 / 38	SW	1522	41°11'	34°28'
Çorum, Kargı, Şahinkayası mevkii	SAH	*P. nigra*	12 / 21	S	1300	41°13'	34°47'
Bilecik, Muratdere	ERC	*P. nigra*	12 / 25	SE	1240	39°53'	29°50'
Bolu, Yedigöller, Ayıkaya mevkii	BOL	*P. sylvestris*	10 / 20	SW	1702	40°53'	31°40'
Eskişehir, Mihalıççık, Savaş alanı mevkii	SAV	*P. nigra*	10 / 18	S	1558	39°57'	31°12'
Kayseri, Aladağlar milli parkı, Hacer ormanı	HCR	*P. nigra*	18 / 33	S	1884	37°49'	35°17'
Kahramanmaraş, Göksun, Payanburnu mevkii	PAY	*P. nigra*	10 / 17	S	1367	37°52'	36°21'
Artvin, Borçka, Balcı işletmesi	ART	*Abies nordmanniana Picea orientalis*	23 / 45	N	1200–2100	41°18'	41°54'

592
593

594 Table 2. Summary statistics for the new chronologies developed by this study in Turkey.

| Site Code | Total chronology | | | Common interval | | |
	Time span	1st year (*EPS > 0.85)	Mean sensitivity	Time span	Mean correlations: among radii /between radii and mean	Variance explained by PC1 (%)
KAR	1307–2003	1620	0.22	1740–1994	0.38 / 0.63	41
SAH	1663–2003	1738	0.25	1799–2000	0.42 / 0.67	45
ERC	1721–2008	1721	0.23	1837–2008	0.45 / 0.69	48
BOL	1752–2009	1801	0.18	1839–1994	0.32 / 0.60	36
SAV	1630–2005	1700	0.17	1775–2000	0.33 / 0.60	38
HCR	1532–2010	1704	0.18	1730–2010	0.38 / 0.63	40
PAY	1537–2010	1790	0.18	1880–2010	0.28 / 0.56	32
ART	1498–2007	1624	0.12	1739–1996	0.37 / 0.60	41

595 *EPS = Expressed Population Signal [Wigley et al., 1984]

596

597 Table 3. Principal components analysis statistics for the Turkey temperature reconstruction
598 model.

	Explained variance	Correlation coefficients with		The chronologies represented by higher magnitudes** in the eigenvectors
	(%)	May–August PPT	March–April TMP	
PC1	46.57	0.65	0.19	KAR, KIZ, TEF, BON,USA,TUR, CAT, INC, ERC, YAU, SAV, TAN, SIU
PC2	7.86	–0.07	0.15	KAR, SAV, TIR, BOL, YAU, ESK, TEF,BON, SIU
PC3*	4.93	0.04	–0.48	HCR, PAY, BOL, YAU, SIA
PC4*	4.68	0.11	0.17	TEF, KEL, FIR, SIA, KIZ, SIU, ART
PC5*	4.42	–0.25	0.27	SAH, TIR, FIR, ART
PC6	3.73	0.15	–0.14	KIZ, FIR, SAV, KAR, TIR, PAY, ESK, TEF, BON, ART
PC7*	3.56	0.19	0.18	KIZ, BON, BOL, YAU, HCR, PAY, INC
PC8	2.87	0.26	0.01	HCR, ESK, BON, FIR, ERC, SIA
PC9*	2.45	0.16	0.17	PAY, USA, BOL, YAU, TIR, HCR, FIR, SIA, SIU
PC10*	2.21	0.14	–0.08	TUR, CAT, SAV, SIA, KEL, ERC, SIU
PC11	2.09	–0.36	–0.20	HCR, TEF, USA, INC, PAY, TUR, SAV, SIU
PC12	1.80	–0.12	0.05	TEF, CAT, YAU HCR, ESK, USA, BOL, SIA
PC13	1.63	–0.06	0.17	TEF, TUR, BOL, KAR, YAU, SIA
PC14	1.55	–0.14	0.06	TIR, USA, FIR, TUR, YAU, KAR, BON
PC15*	1.50	–0.20	–0.14	KIZ, BON, USA, ESK, INC, BOL
PC16	1.31	0.04	0.08	SAH, HCR, INC, YAU, SAV, KAR, FIR, BOL, SIU
PC17*	1.25	0.15	0.19	SAH, SIU, KAR, ESK, TUR, ERC
PC18	1.14	0.13	0.02	KAR, TEF, TUR, SAV, BON, CAT
PC19	1.09	0.16	–0.11	PAY, INC, SAV, HCR, KEL, CAT, TAN
PC20	0.95	–0.15	–0.01	TIR, SAH, CAT
PC21*	0.89	0.06	–0.28	TUR, INC, TIR, SAV
PC22	0.85	0.44	0.10	KIZ, SAH, BON, YAU, SIU
PC23	0.67	–0.22	–0.02	TAN, KEL, TUR, CAT

599   "*" indicates the PCs, which used in the reconstruction as predictors

600   "**" which exceed ±0.2 value.

601

602

603

604

605

606 Table 4. Calibration and verification statistics of bootstrap method (1000 iterations

607 applied) showing the mean values based on the 95% confidence interval (CI).

608

		Mean (95% CI)
Calibration	RMSE	0.65 (0.52; 0.77)
	R^2	0.73 (0.60; 0.83)
Verification	RE	0.54 (0.15; 0.74)
	CE	0.51 (0.04; 0.72)
	RMSEP	0.88 (0.67; 1.09)

609 *RMSE* root mean squared error; R^2 coefficient of determination; *RE* reduction of error; *CE*

610 coefficient of efficiency; *RMSEP* root mean squared error prediction

611

612 Table 5. Calibration and cross-validation statistics for the Turkey temperature reconstruction
613 model.

Calibration Period	Verification Period	Adj. R^2	F	RE	CE
1930–1966	1967–2002	0.55	5.91	0.64	0.58
			$p < 0.0001$		
1967–2002	1930–1966	0.71	10.45	0.63	0.46
			$p < 0.0001$		

614

615

616
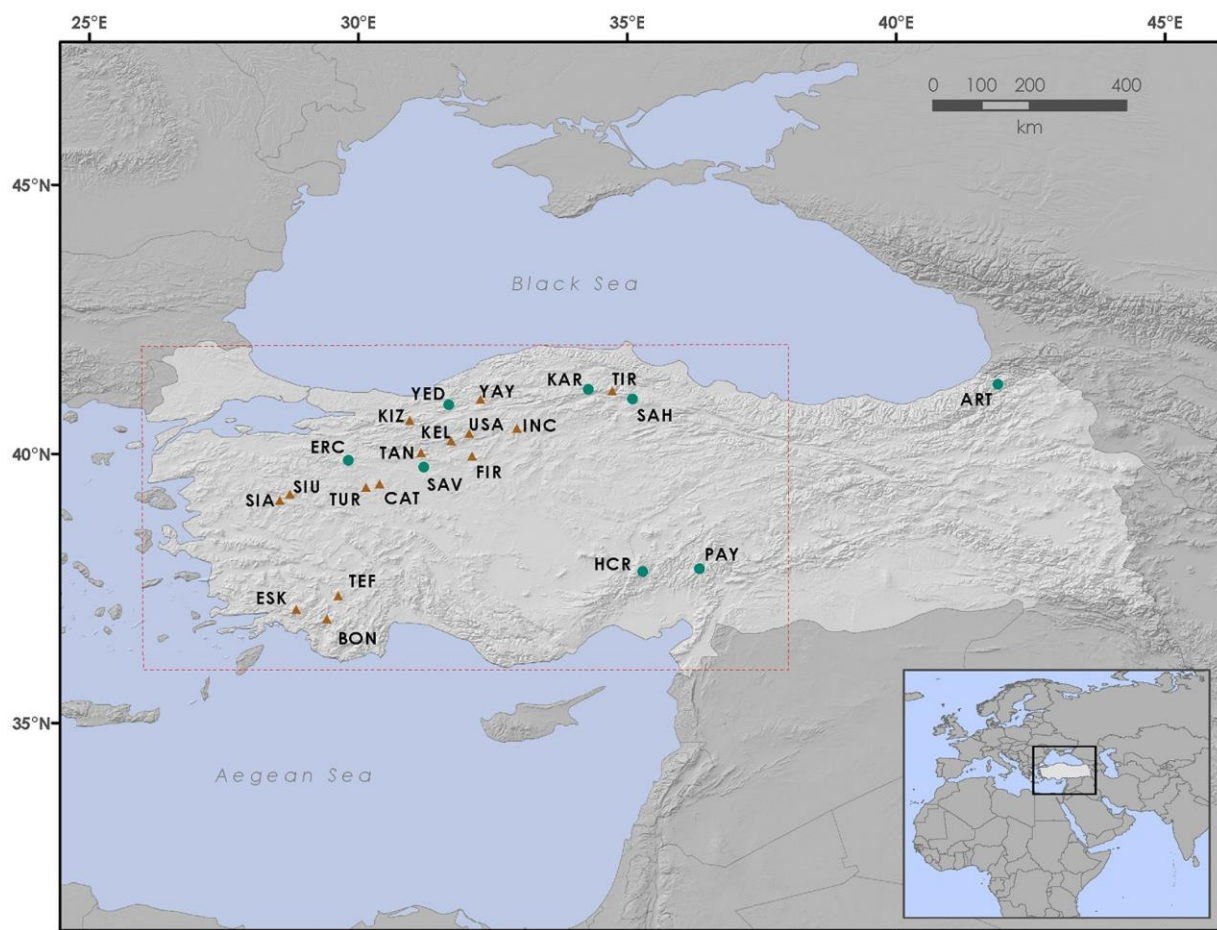
617
618 **Figure 1.** Tree-ring chronology sites in Turkey used to reconstruct temperature. Circles

619 represent the new sampling efforts from this study and the triangles represent previously-

620 published chronologies (YAY, SIA, SIU: Mutlu et al. 2011; TIR: Akkemik et al. 2008; TAN:

621 Köse et al. unpublished data; KIZ, ESK, TEF, BON, KEL, USA, FIR, TUR: Köse et al. 2011;

622 CAT, INC: Köse et al. 2005). The box (dashed line) represents the area for which the

623 temperature reconstruction was performed.

624

625

626

627
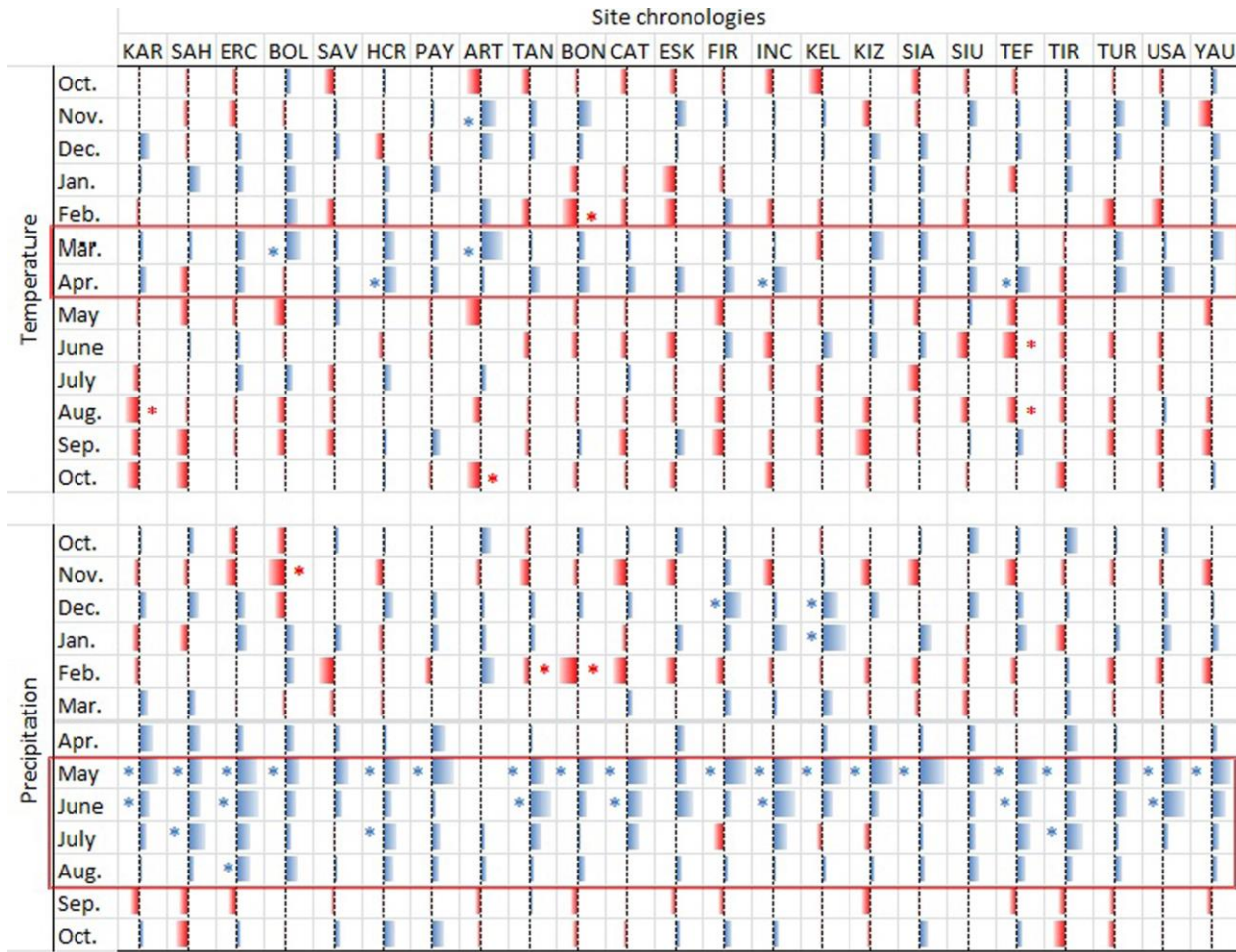
Figure 2. Summary of response function results of 23 chronologies. Red color represents

negative effects of climate variability on tree ring width; blue color represents positive effects of

climate variability on tree ring width. "*" indicates statistically significant response function

confidents ($p < 0.05$). Each response function includes 13 weights for average monthly

temperatures and 13 monthly precipitations from October of the prior year to October of current

year.

634
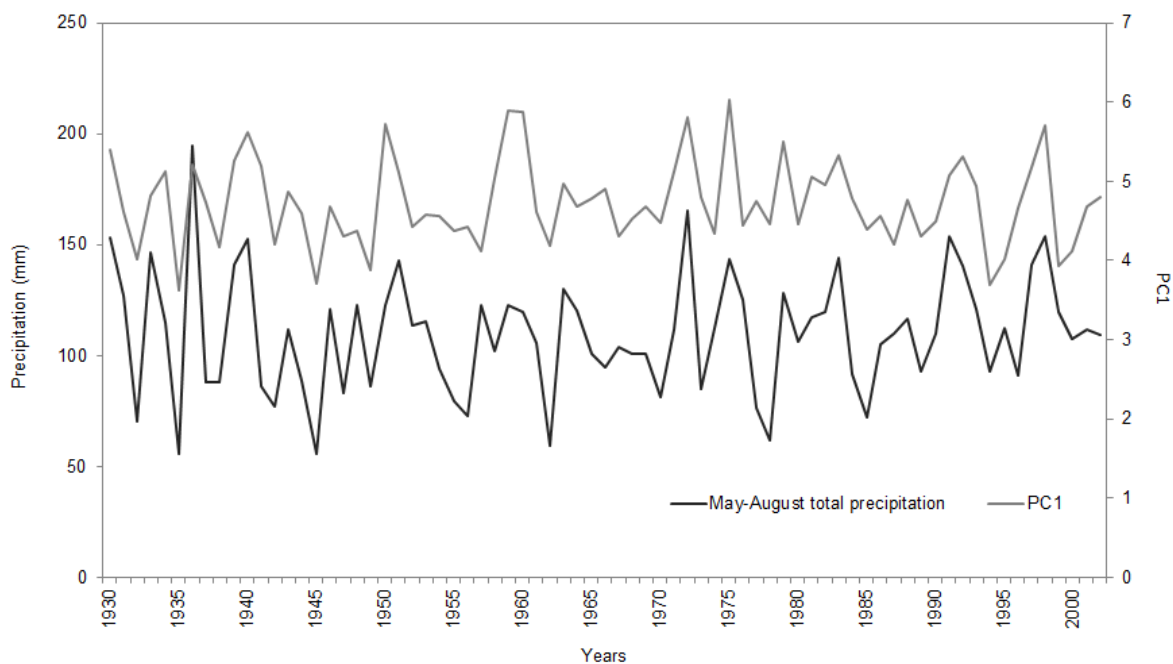
635   **Figure 3.** The comparison of May–August total precipitation (black) and the first principal

636   component of 23 tree-ring chronologies (gray). Correlation coefficient between two time series is

637   0.65 ($p < 0.001$).

638

639

640

641
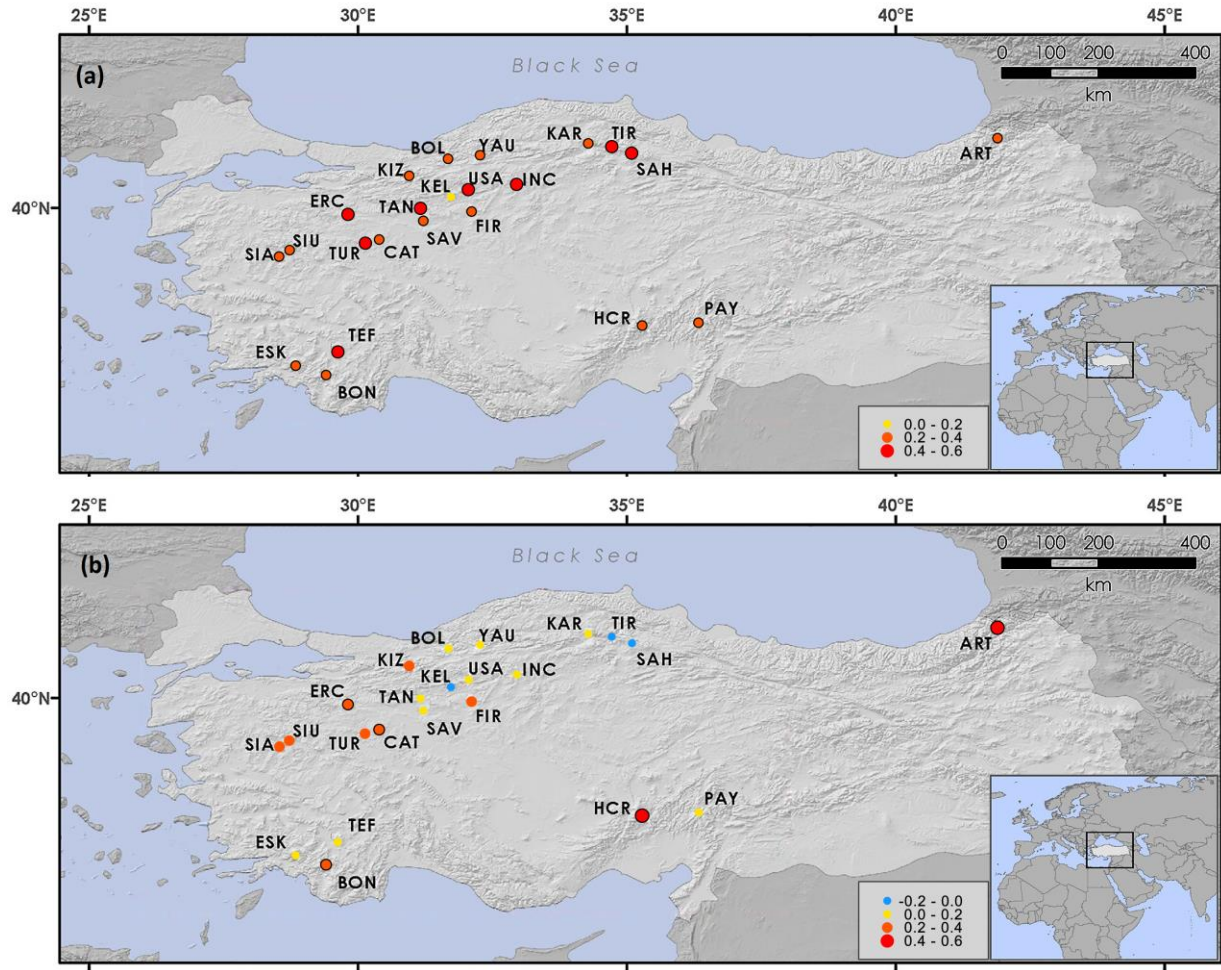
Figure 4. Maps showing Pearson's correlation coefficients between the sites chronologies and

(a) May–August total precipitation and (b) March-April mean temperature for the period 1930–

2012. For each site, the closest gridded (0.5° x 0.5°) climate data obtained from CRU dataset

were used. Graduated circle size and color correspond to correlation coefficient versus the

climate variable. Black lines surrounding circles represent significant correlation coefficients (p

< 0.05).

648

649

650

651

652
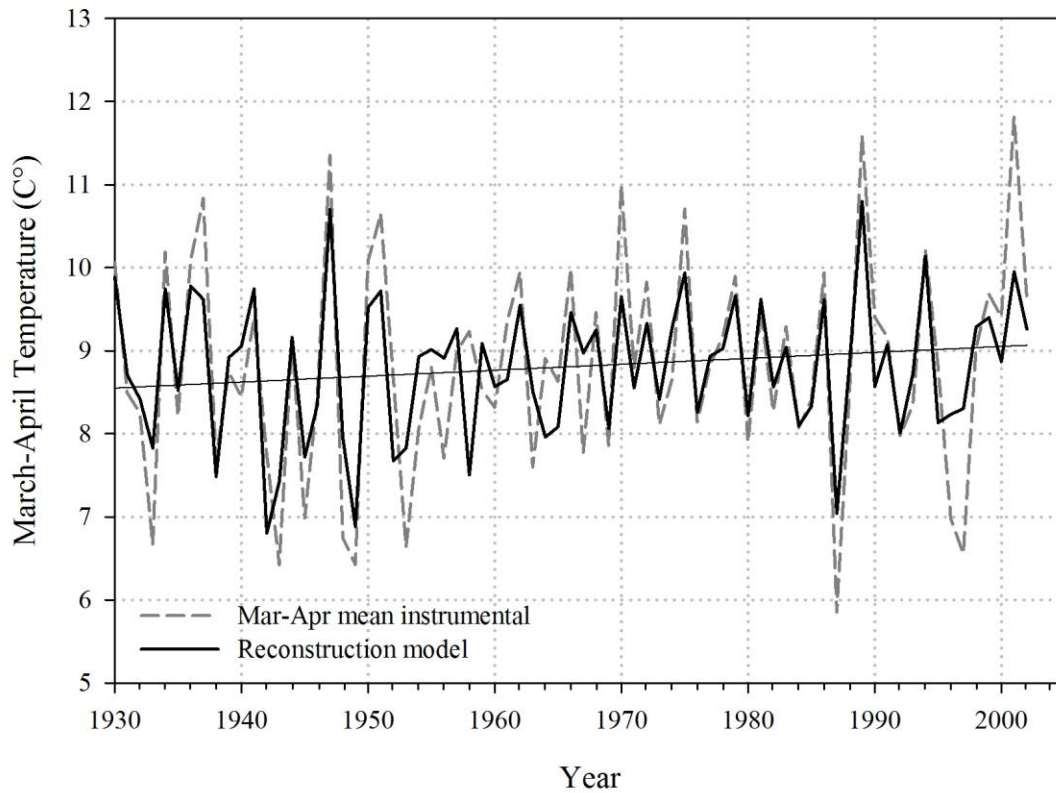
653 **Figure 5.** Actual (instrumental) and reconstructed March–April temperature (°C). Dashed lines

654 (dark grey) represent actual values and solid lines (black) represent reconstructed values shown

655 with trend line (linear black line). Note: y-axes labels range 5–13 °C.

656

657

658

659

660

661

662

663
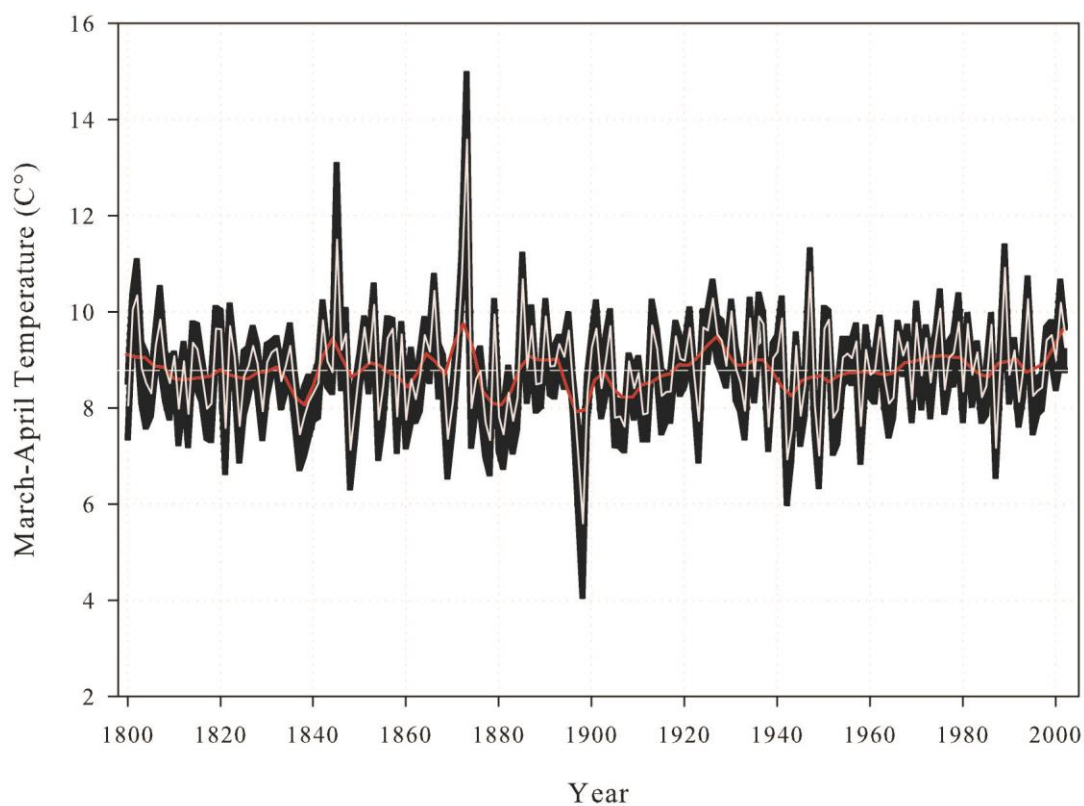
664

665 **Figure 6.** March–April temperature reconstruction for Turkey for the period 1800–2002

666 CE. The central horizontal line (dashed white) shows the reconstructed long-term mean;

667 black background denotes Monte Carlo ($n = 1000$) bootstrapped 95% confidence limits;

668 and the red line shows 13-year low-pass filter values. Note: y-axis labels range 2–16 °C.

669

670

671

672

673
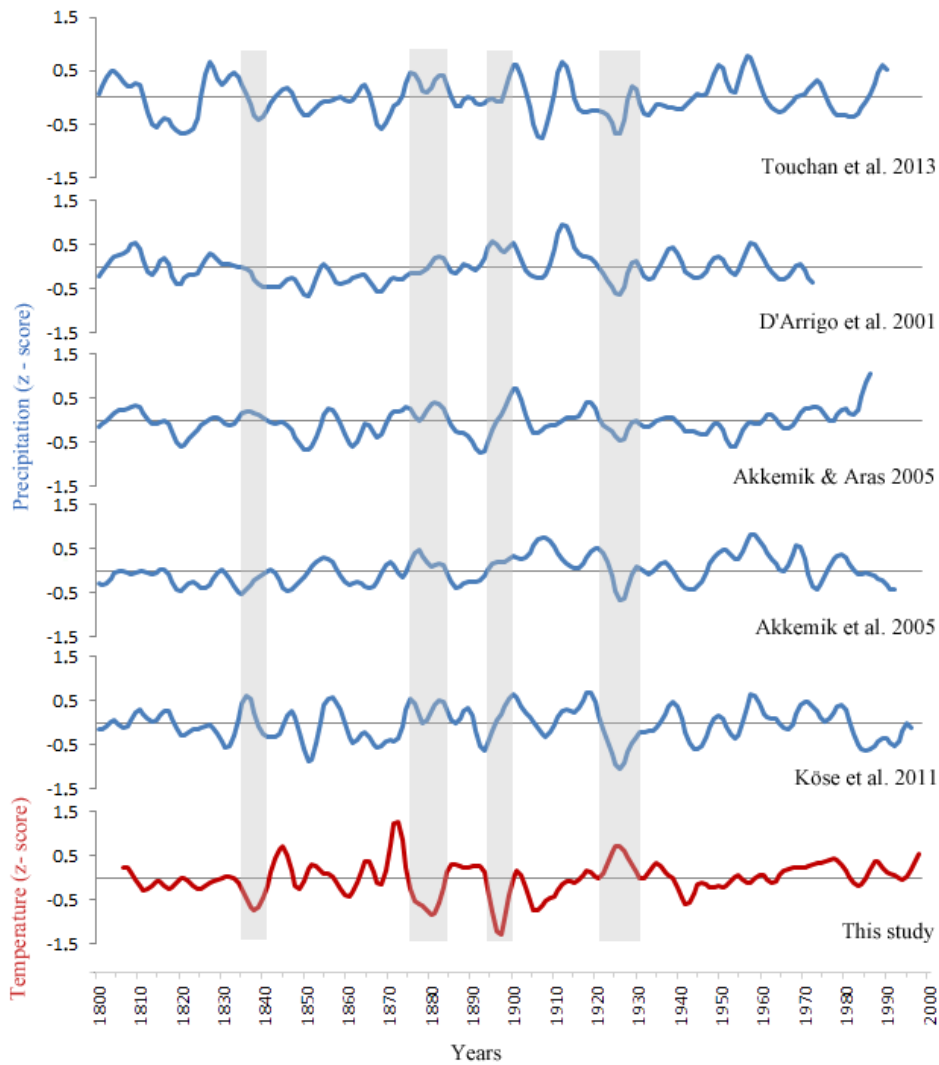
Figure 7. Low-frequency variability of previous tree-ring based precipitation

reconstructions from Turkey and spring temperature reconstruction. Each line shows 13-

year low-pass filter values. z-scores were used for comparison.

677
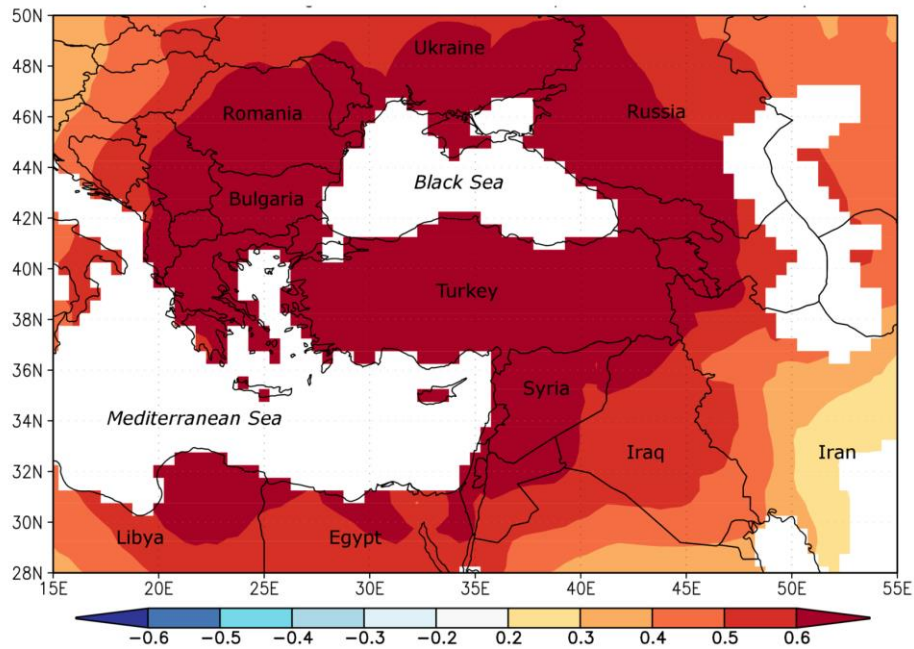
Figure 8. Spatial correlation map for the March–April temperature reconstruction. Spatial

field correlation map showing statistical relationship between the temperature

reconstruction and the gridded temperature field at 0.5º intervals (CRU TS3.23; Jones and

Harris 2008) during the period 1930–2002 over the Mediterranean region. For each grid,

calculated correlation coefficient from 0.20 to 0.60 is significant ($p < 0.05$).

683

684
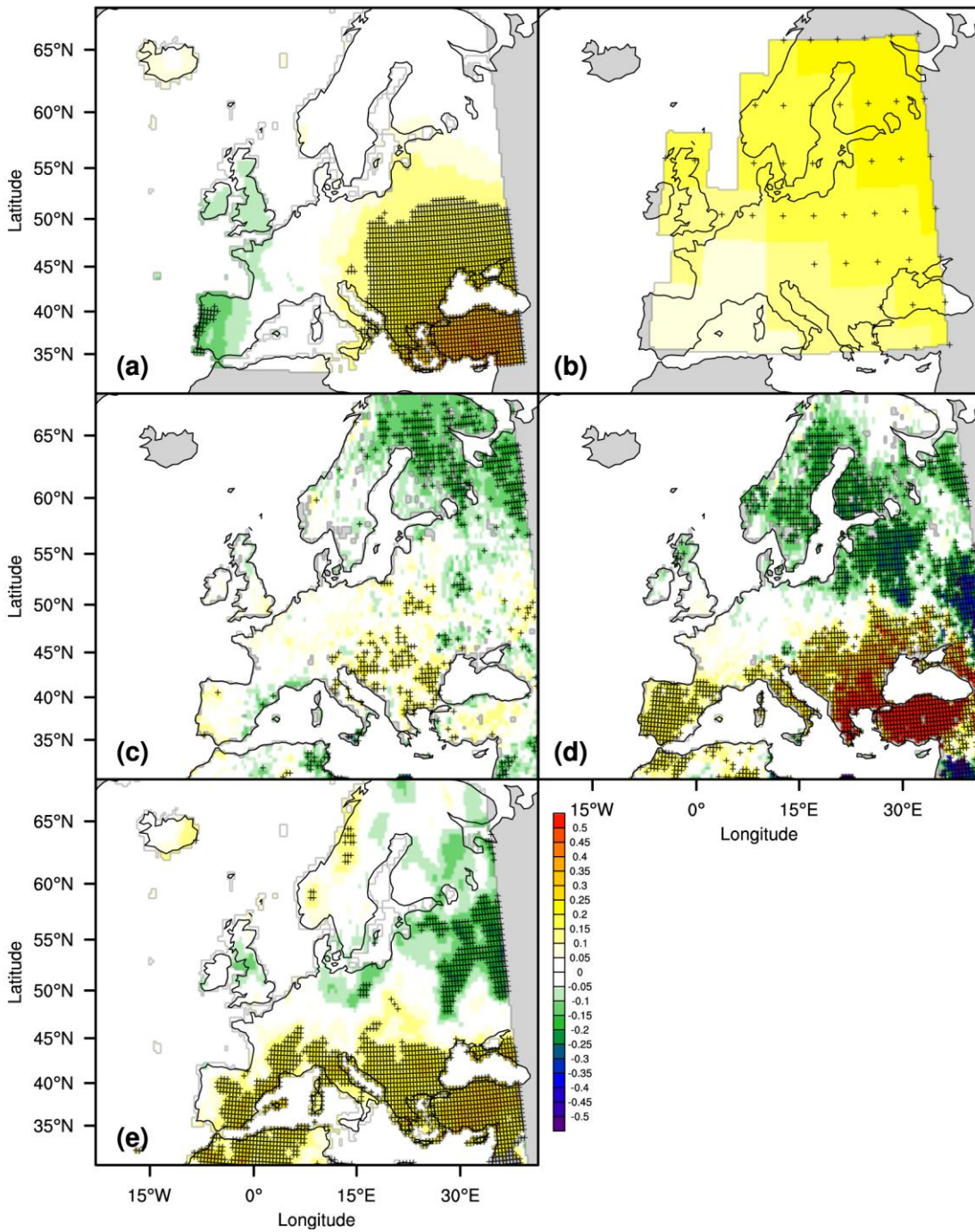
Figure 9. Spatial correlation maps for the March–April temperature reconstruction and

precipitation signal (PC1) obtained from tree-ring data set during the period 1800–2002

over Europe. Maps demonstrate spatial field correlations between our temperature

688   reconstruction and (a) gridded spring temperature reconstruction for Europe (Xoplaki et al.

689   2005), (b) gridded summer temperature reconstruction for Europe (Luterbacher et al. 2016), (c)

690   Old World Drought Atlas (OWDA; Cook et al. 2015). Panels (d) and (e) show spatial

691   correlations between PC1 and OWDA (Cook et al. 2015) and gridded European summer

692   precipitation reconstruction (Pauling et al., 2006), respectively. '+' represents significant

693   correlation coefficients ($p < 0.05$).

694

695
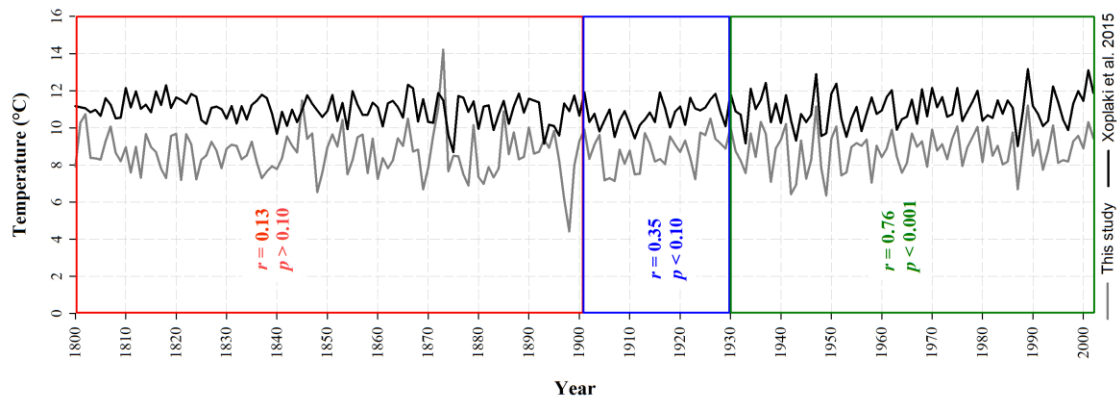
696   **Figure 10.** Comparison of March-April temperature reconstruction (gray) with the mean of

697   corresponding grid points from European spring (March to May) temperature reconstruction

698   (Xoplaki et al. 2005; black) over the study area (36–42º N, 26–38º E). The indicated correlation

699   coefficients are calculated for instrumental period (also calibration period for this study) (1930–

700   2002; $r = 0.76$, $p < 0.001$); for the pre-instrumental period of Turkey, while instrumental data has

701   sufficient quality for most part of Europe (1901–1929; $r = 0.35$, $p < 0.10$); and for pre-

702   instrumental period (1800–1900; $r = 0.13$, $p < 0.10$).

703

704